Journal of Structural Geology, Vol. 9, No. 4, pp. 491 to 500, 1987
Printed in Great Britain

0191-8141/87 $03.00 + 0.00

Structural/stratigraphic models for extensional basins of half-graben type

DAVID BARR*

British Geological Survey, 19 Grange Terrace, Edinburgh EH9 2LF, U.K.

(*Received* 2 *June* 1986; *accepted in revised form* 27 *October* 1986)

Abstract—The equations describing subsidence in isostatically compensated basins formed by lithospheric stretching can be modified to define a 'notional depth to decollement', which relates subsidence to the stretching factor β in much the same way as the depth to a physical sole fault relates subsidence to extension in uncompensated (thin-skinned) basins. For a constant-density basin fill, this notional depth to decollement corresponds to the level of no vertical motion within the lithosphere. In general, the physical sole to a system of detached normal faults will not lie at the notional depth to decollement and must move vertically during extension. This vertical movement must be implicitly corrected for before area/bed length balancing is used to determine the depth to a physical sole fault.

The notional depth to decollement has been calculated numerically for an extensional basin loaded by sediments which follow a North Sea 'shaly sand' compaction law, and increases with β from 5 to 9 km. A set of model half-grabens has been constructed by combining subsidence curves generated by this 'shaly sand' model with geometric relationships inherent in the rotated planar ('domino') mechanism of upper crustal faulting. For comparison, a similar set of half-grabens was constructed for an uncompensated basin with a sole fault at 7.5 km depth. In both cases, large fault-to-fault spacings give rise to large basement relief and consequent footwall uplift and erosion. Small fault spacings give rise to simple listric growth faults. Intermediate values generate more complex uplift/subsidence histories, which are capable of giving rise to such commonly observed features as rounded (eroded) fault-block shoulders, local regression followed by onlap, or 'exponentially' increasing subsidence at the crest of the fault block.

INTRODUCTION

IN RECENT years it has become increasingly clear that subsidence over passive continental margins, and in most sedimentary basins other than flexural foreland basins associated with orogenic belts, is primarily a consequence of crustal thinning and, by inference, extension. According to the model of McKenzie (1978), instantaneous whole-lithosphere stretching gives rise to a rapid stage of initial or tectonic subsidence, in which the basin fill of water or low-density sediments is isostatically compensated by elevation of the Moho and displacement of continental crust by higher-density mantle (Fig. 1). The upper crust appears to deform in a brittle fashion above an intracrustal decollement, so that reflection seismic sections in areas of lithospheric stretching characteristically show tilted basement fault blocks separated by asymmetric, sediment-filled half-grabens (e.g. Montadert *et al.* 1979, Gibbs 1984). Thermal re-equilibration of the lithosphere takes place on a time-scale of the order of 100 Ma, significantly longer then the duration of most stretching episodes (Parsons & Sclater 1977, McKenzie 1978), so the base of the lithosphere is also elevated during stretching (Fig. 1), isotherms are compressed and heat flow increases within the basin. A phase of near-exponential 'regional' or 'thermal' subsidence follows stretching as heat flow declines and the thermally defined base of the lithosphere returns to its equilibrium level. Sediments deposited during this period are comparable in thickness to those deposited during stretching (e.g. Le Pichon & Sibuet 1981), but marker horizons are unextended and drape the fault-blocks produced during extension (e.g. Badley *et al.* 1984). The basic McKenzie model can be modified to allow for factors such as non-instantaneous or inhomogeneous stretching, 'basification' of crust by intrusion of mafic magma, a convective component of heat transfer and delamination of mantle lithosphere. Various forms of the stretching model have been applied to sedimentary basins in a wide variety of tectonic and geographic settings (e.g. McKenzie 1978, Steckler & Watts 1978, Jarvis & McKenzie 1980, Sclater & Christie 1980, Royden & Keen 1980, Le Pichon & Sibuet 1981, Hellinger & Sclater 1983, Cochran 1983, Royden *et al.* 1983, Barton & Wood 1984).

Models of inhomogeneous (e.g. two-layer) stretching require the differentially extended layers to be separated by a gently dipping decollement, and also require excess

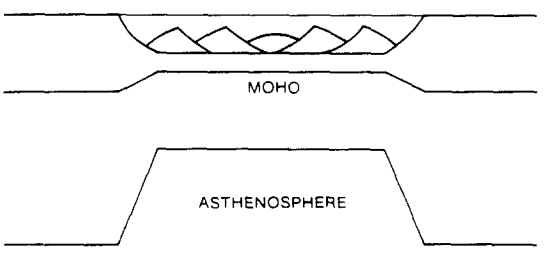

Fig. 1. Schematic model of stretched continental lithosphere, prior to thermal subsidence. The lower crust and mantle have been deformed by ductile flow, while the brittle upper crust has been deformed by detached normal faulting.

*Present address: Britoil plc, 301 St Vincent Street, Glasgow G2 5DD, U.K.

upper-plate extension in one geographic area to be linked with excess lower-plate extension in another, in order that a lithosphere-scale cross-section can be balanced in the sense of Dahlstrom (1969) and Gibbs (1983). The latter requirement holds even if the decollement is not horizontal as shown in Fig. 1, but dips at a moderate angle and penetrates the entire lithosphere as a through-going shear zone (cf. Wernicke 1981, 1985). The complex interplay of upper- and lower-plate stretching can give rise to zones of syntectonic uplift as well as subsidence, and thermal subsidence can be partly or wholly decoupled in a geographic sense from initial (syntectonic) subsidence (e.g. Wernicke 1985, fig. 12). Wernicke (1985) has considered the case of isostatically compensated thin-skinned basins, but it appears that some thin-skinned basins do not achieve local isostatic compensation. Section-balancing constraints require that these too link via a sole fault or basal shear zone to a locus of lower (or whole) lithosphere stretching. Presumably the absence of isostatic compensation is a function of the magnitude of the isostatic imbalance and the flexural rigidity of the local lithosphere—small shallow basins developed in thermally old thick lithosphere are more likely to remain uncompensated than large deep basins in young thin lithosphere. Uncompensated basins can form in a variety of tectonic settings: the Vienna basin (Royden *et al.* 1983), for example, is genetically associated with thin-skinned thrusting, while the Inner Moray Firth pull-apart basin (McQuillin *et al.* 1982, Barr 1985) is located on a major strike–slip fault active during and presumably related to regional extension of the U.K. continental shelf. Uncompensated basins directly related to extension of a nearby passive continental margin probably include the Tucano Basin of Brazil (Ussami *et al.* 1986) and the basins of the Long Island Platform, offshore New York (Hutchinson *et al.* 1986).

Perfect Airy compensation and total lack of local compensation both require that the lithosphere has zero or infinite flexural thickness and will rarely occur in nature. For example, the Inner Moray Firth basin is partially compensated in its eastern portion (Barr 1985), and the 100 km wide Tucano basin is compensated by a Moho uplift of about 1000 km wavelength (Ussami *et al.* 1986). However, it is useful to consider the two end-member cases, as they make quite different predictions about basin subsidence histories and aspects of fault-block geometry.

SUBSIDENCE DURING STRETCHING

Two end-member types of extensional basin

The most obvious observational difference between compensated and uncompensated basins should lie in their gravity fields: uncompensated basins will show much larger departures from the regional field. Where the sediment–water interface lies close to sea-level, large perfectly compensated basins should have Bouguer and free-air gravity anomalies which average close to zero, while uncompensated basins should be characterised by a negative anomaly whose magnitude can be precisely explained by the density contrast between sediments and laterally adjacent basement (e.g. Donato & Tully 1981). Such basins must of course be flexurally compensated by a widespread low amplitude Moho uplift (i.e. they are compensated on the scale of the lithospheric plate as a whole), but the associated positive gravity anomaly would be indistinguishable from the regional field.

The major tectonic difference between the two types of basin is that uncompensated basins lack the post-stretching thermal subsidence stage (although this can also be a feature of thin-skinned compensated basins, as long as unloading during stretching has not resulted in significant isostatic uplift of the base of the lithosphere). Indeed, uncompensated basins may experience post-stretching uplift as the basin attempts to return to isostatic equilibrium (Barr *et al.* 1985). Because post-stretching thermal subsidence is a consequence of the bunching of isotherms during stretching, it follows that uncompensated basins lack the elevated heat flow which characterises the extensional stage in compensated basins and favours the early generation of hydrocarbons (McKenzie 1978, 1981). Neither of these commercially important differences is addressed by the present paper, which concentrates on aspects of basin geometry during stretching.

In a thin-skinned uncompensated sedimentary basin, it is reasonable to assume that the sole to the normal fault system maintains a constant elevation below a sea-level datum. In cross-section, the area of the basin fill A_1 bears a simple relationship to the extension e and the depth to decollement d (Fig. 2) (Gibbs 1983):

$$A_1 = A_2 = ed. \quad (1)$$

This can also be expressed in terms of the stretching factor β (ratio of deformed to initial length) and the mean depth to the basin floor z (Barr 1987):

$$z = d\,(1 - 1/\beta). \quad (2)$$

For a given stretching factor, a deep decollement will give rise to a deep basin, and a shallow decollement to a shallow basin.

The situation in instantaneously stretched, isostatically compensated basins is rather different. The initial

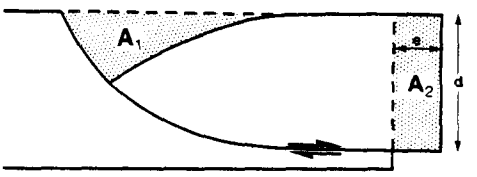

Fig. 2. Cross-section through a thin-skinned basin produced by withdrawing the hangingwall a horizontal distance e above a decollement at depth d and allowing it to collapse onto the bounding fault. Area of sediment fill $A_1 = A_2 = ed$.

tectonic subsidence is given by equation (1) of McKenzie (1978):

$$S_i = \left[\frac{a\left\{(\varrho_0 - \varrho_c)\frac{t_c}{a}\left(1 - \frac{\alpha T_1 t_c}{2a}\right) - \frac{\alpha T_1 \varrho_0}{2}\right\}}{\varrho_0(1 - \alpha T_1) - \varrho_s} \right] \times (1 - 1/\beta). \quad (3)$$

The parameters in square brackets are properties of the continental lithosphere (thicknesses, densities, coefficient of thermal expansion), and sediment loading has been explicitly accounted for by replacing ϱ_w of McKenzie (1978) with ϱ_s, the mean density of the sediment ± water column. If discussion is restricted to continental lithosphere, the top of which lay at sea-level before stretching, and which was in isostatic equilibrium with the mid-ocean ridge system, these parameters are not independent and they combine to yield a constant with units of depth. Barr (1987) showed that the value of this constant is controlled primarily by ϱ_s. The physical significance of this constant can be appreciated from Fig. 3: it corresponds to the depth to which the asthenosphere would rise if loaded by a sediment/water column of mean density ϱ_s (in the water-loaded case, to the 'mantle geoid' of Turcotte *et al.* (1977)). In the case of a sediment-loaded basin, Barr (1987) proposed that this constant be referred to as the 'notional depth to decollement', d_n, in order to emphasis the analogy with equation (2). In a real basin, the magnitude of d_n will increase with β as the sediment column compacts and increases in density.

Equations (2) and (3) express the fundamental difference between (locally) uncompensated and compensated basins: in the former, overall subsidence is closely controlled by the geometry of the upper crustal fault system and particularly its depth to decollement, whereas in the latter, subsidence is essentially independent of this geometry or of the depth to a physical decollement surface, and depends only on global properties of the lithosphere. A corollary is that, unless certain precautions are taken, attempts to determine depth to decollement by area-balancing geoseismic cross-sections (cf. Gibbs 1983) will yield the true depth to decollement in uncompensated basins, but only the notional depth to decollement in compensated basins. In a compensated basin with a constant-density basin fill (e.g. seawater), the notional depth to decollement corresponds to the (unique) level of no vertical motion during stretching. Any physical sole fault which does not lie at this level must move vertically as a passive marker during extension: equations describing this vertical movement are provided by Barr (1987).

Successful prediction of the depth to a physical sole fault by area-balancing cross-sections requires construction of a corrected regional datum from which basin depth or cross-sectional area is measured. This datum represents the elevation to which top basement or some other marker horizon would have been displaced by thermal, isostatic or other regional processes, if the geometric effects produced solely by upper crustal faulting were excluded. In general, this will not simply be a straight line joining basement elevations on either side of the basin, but will have a complex (e.g. bowed) shape and will evolve in space and time, mimicking the behaviour of the sole fault. For example, in Fig. 7 the mean sediment thickness at $\beta = 2$ is 3.65 km, yielding a notional depth to decollement of 7.3 km. Suppose the physical sole fault had initiated at 10 km depth. At $\beta = 2$, it would have been passively uplifted to 8.65 km and so the regional datum should have been constructed at an elevation of 1.35 km above sea-level. The total subsidence relative to datum would then become 5 km, with the depth to the physical sole fault correctly estimated as 10 km below the regional datum. In practice, it will often be difficult or impossible to define this regional datum objectively.

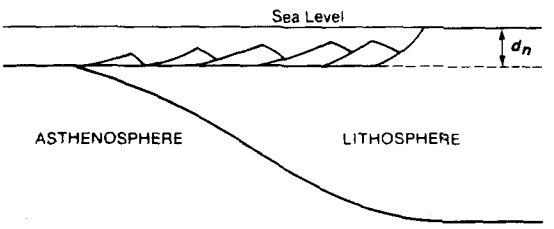

Fig. 3. Schematic water-loaded continental margin showing the physical significance of the notional depth to decollement d_n (the level of no vertical motion or mantle geoid). At infinite extension, $1 - 1/\beta = 1$, the initial subsidence due to stretching $S_i = d_n$, and the asthenosphere is directly overlain by sea-water. Note that although the physical sole to the system of upper crustal fault blocks has been drawn at the notional depth to decollement, this will not generally be the case.

Uplift or subsidence during stretching?

McKenzie (1978) stated that uplift occurs during instantaneous homogeneous lithospheric stretching if the continental crust is thinner than 18 km, and subsidence if it is thicker than 18 km. In a more general discussion, Jarvis (1984) also considered the effect of varying the thickness of the pre-stretching lithosphere. By referring the pre-stretching crustal elevation to the mantle geoid or notional depth to decollement, it is possible to simplify discussion of whether homogeneous lithospheric stretching produces uplift or subsidence. In fact it is not necessary to know the absolute magnitude of any of the parameters in equation (3). The general rule pointed out by Le Pichon *et al.* (1982) is that lithosphere whose pre-stretching surface elevation was deeper than the water- or sediment-loaded mantle geoid is uplifted during stretching, while lithosphere whose pre-stretching elevation was shallower than the mantle geoid subsides during stretching. Because the water-loaded mantle geoid lies at about 3.3 km below sea-level (see compilation by Barr 1987), continental lithosphere can only be uplifted during homogeneous stretching if it had previously undergone severe extension and thermal subsidence to abyssal depths. For a water-loaded basin, this would require that β was greater than two during a stretching episode about 120 Ma earlier than the present one. The earlier stretching factor has to be even larger if

the two stretching episodes are less widely separated in time, or if sediment-loaded thinned crust is to be uplifted (although the top basement surface may be below 3.3 km, the top of the earlier sediment package is likely to be much shallower).

Clearly, there is no possibility of producing regional uplift by homogeneous stretching in an area such as the North Sea, where water depths never exceeded a few hundred metres, or in the East African Rift or the Basin and Range Province of the U.S.A., which were emergent prior to extension. Alternative mechanisms must be sought, such as inhomogeneous stretching, emplacement of asthenospheric diapirs, delamination of mantle lithosphere, small-scale convection in the plastic lower lithosphere, or intrusion of basic magma into the crust (e.g. Royden & Keen 1980, Hellinger & Sclater 1983, Jarvis 1984, McKenzie 1984, Steckler 1985, Yuen & Fleitout 1985). Similarly, extensional uplift of cratonic areas cannot be explained by their low ratio of crustal to lithospheric thickness (e.g. Dewey 1982, pp. 386 and 393). The fact that such areas generally lie close to sea-level rather than several kilometres below sea-level implies that the low crust/lithosphere ratio is compensated for by variations in other parameters such as crustal or mantle density. Syn-stretching subsidence in a craton should be identical to that of any other continental area with a similar pre-stretching elevation, providing of course that isostatic equilibrium was maintained (since the latter is in any case a fundamental assumption of the McKenzie model, this requirement does not further restrict the model's application).

Subsidence of stretched lithosphere whose upper surface lay below sea-level prior to stretching can also be predicted without a knowledge of the individual parameters in equation (3). It is simply necessary to treat the notional depth to decollement as if it were a physical decollement surface situated at a corresponding depth below sea-level. For example, consider a water-loaded basin with a pre-stretching water depth of 0.8 km, stretched by a factor of two. The pre-stretching surface lies (3.3 − 0.8) km = 2.5 km above the notional depth to decollement, so it subsides by 2.5 (1 − 1/2) km = 1.25 km, to a final elevation of (1.25 + 0.8) km = 2.05 km below sea-level. Uplift of lithosphere initially deeper than the notional depth to decollement can be similarly treated, as can subsidence of subaerially extended lithosphere, but in the latter case account has to be taken of the change in subsidence rate when the basin changes from being air-loaded to water-loaded (Jarvis 1984, p. 18).

MODELLING OF UPPER CRUSTAL HALF-GRABENS

Basement geometry

The preceding section provides a rationale for predicting the overall subsidence history of a basin, referred only to the stretching factor β and not to the physical properties of the local lithosphere (assuming subsidence

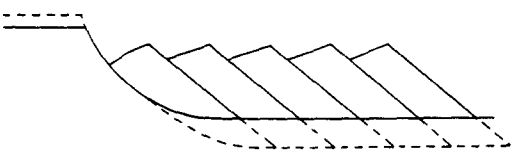

Fig. 4. Schematic representation of a set of rotated planar ('domino') faults. The fault blocks rotate during extension, and some ductile deformation is required at the base of each. Two alternative graben margin/sole fault pairs are shown (by solid and broken lines) to make the point that the geometry of the top basement surface is independent of the depth to decollement, and only its mean elevation varies (i.e. the geometry of each rigid saw-tooth depends only on its apical angle and the amount of rotation).

to start from sea-level). In order to model syntectonic stratigraphic relationships, it is necessary to make some assumptions about the geometry of upper crustal faulting. Several models are available, involving both listric and planar fault geometries (e.g. Wernicke & Burchfiel 1982, Jackson & McKenzie 1983, Chenet *et al.* 1983, Le Pichon *et al.* 1983). Listric faults are difficult to model quantitatively, mainly because there is as yet little agreement on how their hangingwalls deform internally (cf. Gibbs 1983, Chapman & Williams 1984, Bosworth 1985, Gibbs 1985). In contrast, the rotated planar or 'domino' fault model (Figs. 4 and 5) permits precise prediction of the variation of upper crustal geometry with β (Le Pichon & Sibuet 1981, Wernicke & Burchfiel 1982). Fault blocks are considered to be rigid, except for a diffuse accommodation zone near the sole fault, and it is a geometric requirement that they all move simultaneously. A major advantage from the point of view of predictive modelling is that (within certain limits), the *shape* of the top basement surface is independent of the depth to decollement—only the mean depth to the basin floor and the length/width ratio of the dominoes are changed (Fig. 4). The domino fault model gives rise to greater structural relief than models that permit extensive hangingwall deformation, and defines one end-member of the range of possible half-graben geometries. While its precise predictions probably can not be extrapolated to real sedimentary basins, it should nevertheless be possible to draw some general conclusions about the factors controlling half-graben geometry.

The shape of the dominoes in Fig. 5 is defined by the initial fault-plane dip ϕ_i and spacing a', and by the

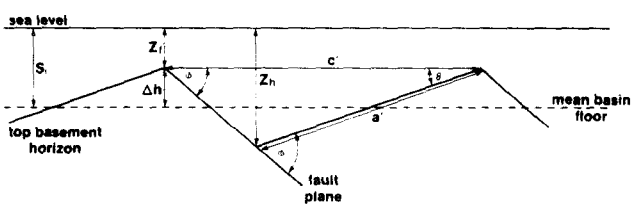

Fig. 5. Detail of the top basement surface in a system of domino faults. S_i is the initial subsidence due to stretching; z_f and z_h the elevations of footwall and hangingwall cutoffs, respectively; a' and c' the pre- and post-stretching fault block spacing; ϕ and ϕ_i the present-day and initial fault-plane dip; and θ the dip of the top basement surface.

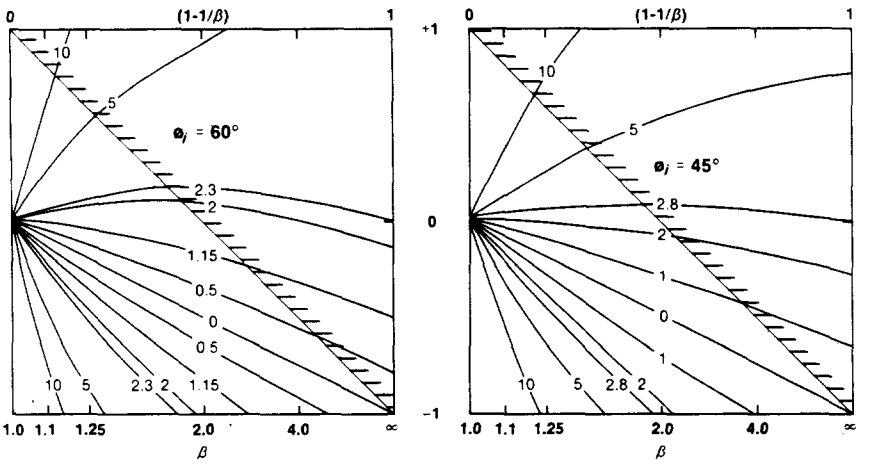

Fig. 6. Sets of curves illustrating footwall uplift/subsidence and hangingwall subsidence in a system of rotated planar ('domino') faults with initial fault-plane dip $\phi_i = 60$ and 45° (Barr in press, fig. 16). All linear dimensions are expressed in terms of the depth to decollement, i.e. the vertical scale ranges from one depth-to-decollement unit above sea-level to one depth-to-decollement unit below sea-level, and the footwall/hangingwall uplift/subsidence curves correspond to initial fault-plane spacings ranging up to 10 times the depth to decollement. The hatched line represents the point at which the domino geometry breaks down. See text for further explanation.

stretching factor $\beta = c'$ (present-day fault spacing) $\div a'$. The present-day fault-plane dip is represented by ϕ, and the maximum height of the basement footwall cutoff above the mean basin floor is given by:

$$\Delta h = 0.5a' \sin \theta,$$

where θ is the dip of the top basement surface. The height of the basement footwall cutoff is one of the most important parameters controlling sedimentation in half-grabens: if it is greater than the mean depth to the top basement surface, footwall islands will be potentially emergent and undergo erosion during extension.

Figure 6, taken from Barr (1987), shows how footwall and hangingwall cutoffs move vertically during the formation of an uncompensated basin. Two sets of curves are presented, for initial fault-plane dips of 60 and 45°; and all linear dimensions are scaled in terms of the depth to the physical sole fault. The labels on the curves represent the initial fault-plane spacing a' (as a multiple of the depth to decollement), and that for $a' = 0$ corresponds to the mean basin floor. The vertical scale is in multiples of the depth to decollement, with 0 representing sea-level. For example, if the sole fault lay at a depth of 10 km below sea-level, Fig. 6 would be read with a vertical scale ranging from 10 km above sea-level to 10 km below sea-level, and the largest initial fault spacing plotted would be 100 km. Closely spaced fault blocks never rise above sea-level, but initial fault spacings greater than 1.15 times the depth to decollement ($\phi_i = 60°$) or twice the depth to decollement ($\phi_i = 45°$) are sufficient to cause uplift of footwall cutoffs above sea-level at low to moderate values of β. For a given initial fault spacing, greater footwall uplift results from a steeper initial fault-plane dip. Considerable ductile strain is required to rotate fault blocks which are significantly wider than the depth to the physical decollement, but the fact that even broad fault blocks can display an essentially domino-like, saw-tooth top basement surface on seismic sections (e.g. Montadert *et al.* 1979, Le Pichon & Sibuet 1983) suggests that strain is concentrated in the deeper parts of the fault blocks and that the geometry of Fig. 5 is not seriously incorrect. Nevertheless, the magnitude of the space problem to be overcome suggests that large-scale footwall uplift will be relatively uncommon in uncompensated basins, particularly if initial fault plane dips are less than 60°.

A comparable set of uplift and subsidence curves can be constructed for an isostatically compensated, homogeneously stretched basin. Those presented in Fig. 7 are also taken from Barr (1987) and were derived numerically for a basin in which the sediment fill follows the North Sea 'shaly sand' compaction law determined by Sclater & Christie (1980), i.e.

$$f = 0.56 \exp(-0.39z),$$

where f is the porosity at a depth of z kilometres below sea-level. The upper panels show how the mean density of the sediment fill ϱ_s increases with β from 1.74 to 2.43 gcm^{-3}, and how fault-plane dip ϕ and bedding-plane dip θ vary for initial fault-plane dips of 60 and 45°. In the lower two panels, the upper heavy curve tracks the elevation of the mean basin floor and the lower heavy curve the notional depth to decollement, both relative to sea-level at 0 km. Note how the notional depth to decollement increases with β from about 5 km to about 9 km, and lies at 7–8 km below sea-level for moderate values of β. The broken curves follow the passive uplift or subsidence of three physical decollement surfaces, initiated at 2.5, 5 and 10 km below sea-level. The numbered curves track hangingwall cutoffs (lower set) and footwall cutoffs (upper set), the labels representing the initial fault-plane spacing a' in kilometres. Critical values for uplift above sea-level are 5.7 km ($\phi_i = 60°$) and 9.9 km ($\phi_i = 45°$). Initial fault spacings in excess of about 10–15 km are

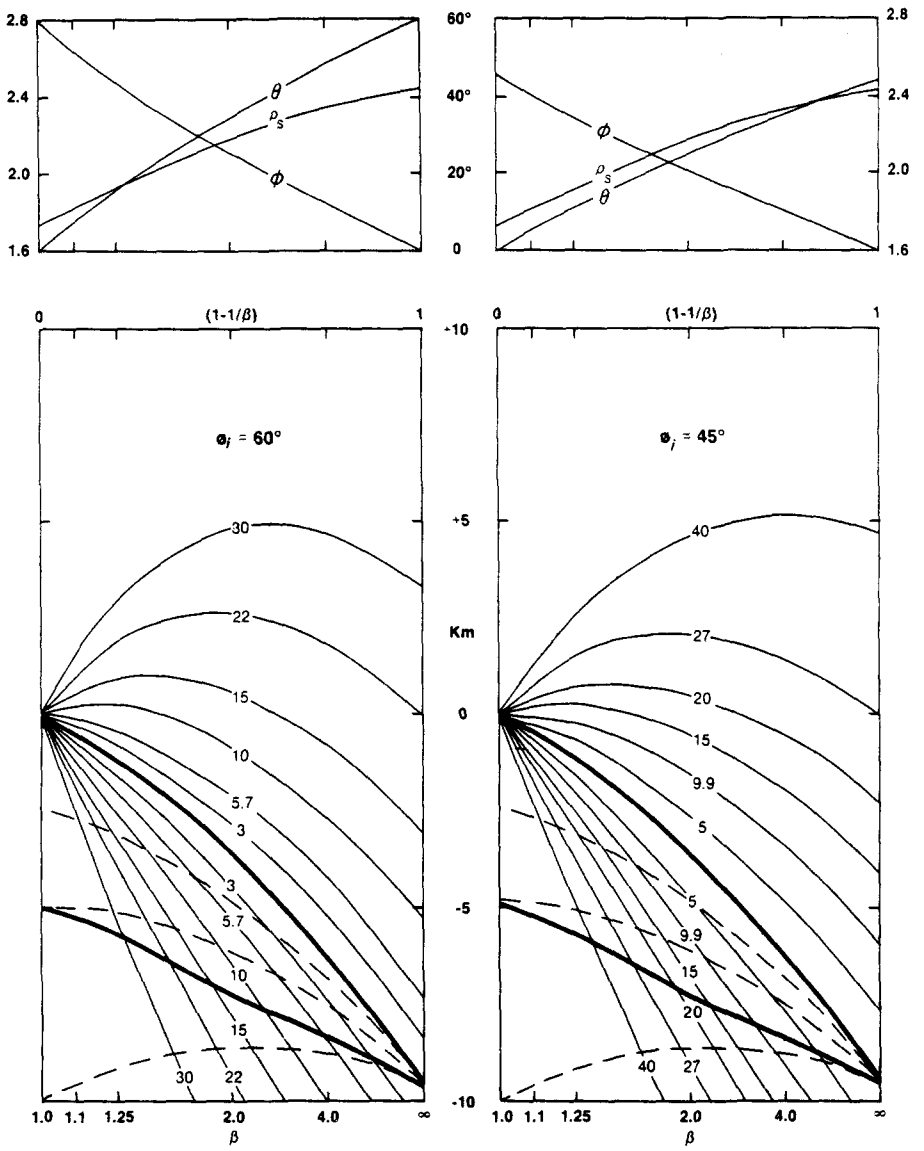

Fig. 7. Sets of curves illustrating footwall uplift/subsidence and hangingwall subsidence in a system of rotated planar ('domino') faults with initial fault-plane dip ϕ_i = 60 and 45°, for an isostatically compensated basin loaded by sediments which follow an exponential 'shaly sand' compaction law (Barr 1987, fig. 7). See text for further explanation.

sufficient to cause significant (hundreds of metres) uplift of footwall cutoffs above sea-level. Accelerating overall subsidence, driven by the increasing sediment density, restricts footwall uplift to lower values of β than in a comparable uncompensated basin (cf. Figs. 6 and 7). Because the depth to the physical sole fault may be much greater than the notional depth to decollement (e.g. 20 km vs 7 km), the space problem associated with wide, short dominoes is less likely to be encountered in a compensated basin, and footwall uplift should be more widespread. Note that this mechanism achieves footwall uplift with rigid fault blocks, and so contrasts with the isostatic footwall uplift mechanism of Jackson & McKenzie (1983), which involves flexing of individual fault blocks. There is some doubt about the applicability of their local isostatic model to small fault blocks within basins (Barr *et al.* 1985), but in general it would magnify the uplift shown in Fig. 7.

Sediment infill

In this section, some simple models are presented for the stratigraphic evolution of extensional half-grabens. Three basic assumptions are made: (1) that upper crustal fault geometry approximates to the domino model; (2) that emergent footwalls are eroded down to sea level; and (3) that basins are filled with sediment to sea-level. The assumption that emergent footwall islands are continuously eroded means that subsidence of footwalls below sea-level commences not at the zero-crossing of each footwall uplift curve in Figs. 6 and 7, but near the crest or maximum turning point (this is a slight over-simplification—see Barr (1987) for a fuller explanation). In uncompensated basins, this crest lies at a relatively high value of β (Fig. 6), so, in a typical basin with β = 1.5–2, most footwalls will record either continuous uplift (at a decreasing rate) or continuous subsidence (at

an increasing rate). In contrast, many footwalls in compensated basins with β = 1.5–2 will have passed the crests of their uplift curves and will therefore record uplift followed by subsidence (Fig. 7). The compensated model is probably more appropriate to large sedimentary basins such as the North Sea and to passive continental margins, so its evolution will be discussed in more detail.

Compensated basins. The models presented take as a starting point the uplift/subsidence curves of Fig. 7, with an initial fault-plane dip of 60°, and will therefore be of most relevance to basins formed by broadly uniform lithospheric stretching and filled near to sea-level with clastic sediments. It is re-emphasised that they apply only to the active extensional stage of basin formation: in an area such as the North Sea, where stretching ceased in the Early Cretaceous, they would be buried beneath a few kilometres of 'sag-basin' sediments deposited during thermal subsidence.

Figure 8 shows the procedure by which each model half-graben was built up, in this case for an initial fault spacing of 10 km. Four increments of extension were used, each corresponding to a rotation of 8–10° and yielding 'freeze-frames' at β = 1.1, 1.25, 1.5 and 2.0. The notional depth to decollement increases from about 5 km at β = 1 to about 7.5 km at β = 2 (Fig. 7). Three basement faults are shown, to depict one complete half-graben and part of each flanking half-graben. Emergent fault blocks have been eroded down to sea-level, and the half grabens filled with sediment. At each stage, the sea-level reference is adjusted so that the total sediment area within each half-graben is equal to the product of the fault spacing c' and the initial subsidence S_i; in other words, the mean basin depth, measured over a distance greater than or equal to the half-graben spacing, is equal to S_i. The model assumes that isostatic compensation takes place on a horizontal scale greater than one fault-block width. That this can be the case in an area of active extension and high heat flow is confirmed by the data of Froidevaux (1986) from the Basin and Range Province, U.S.A. Individual basins and ranges of 20–50 km wavelength are not locally compensated, but regional topography of about 200 km wavelength is.

From area-balance constraints, the depth below sea-level of the basement hangingwall cutoff can be shown to be:

$$z_h = S_i + \tfrac{1}{2}a' \sin \theta,$$

where the basement footwall cutoff is below sea level, or

$$z_h = \sqrt{(2S_i \cdot a' \cdot \sin \theta)},$$

where the footwall cutoff is above sea-level (see Fig. 5 for definition of terms). The sea-level marker is carried forward into the next stage to form a bedding plane within the syntectonic sediments: at each stage, its geometry is modified to take account of sediment compaction according to the 'shaly sand' law discussed above.

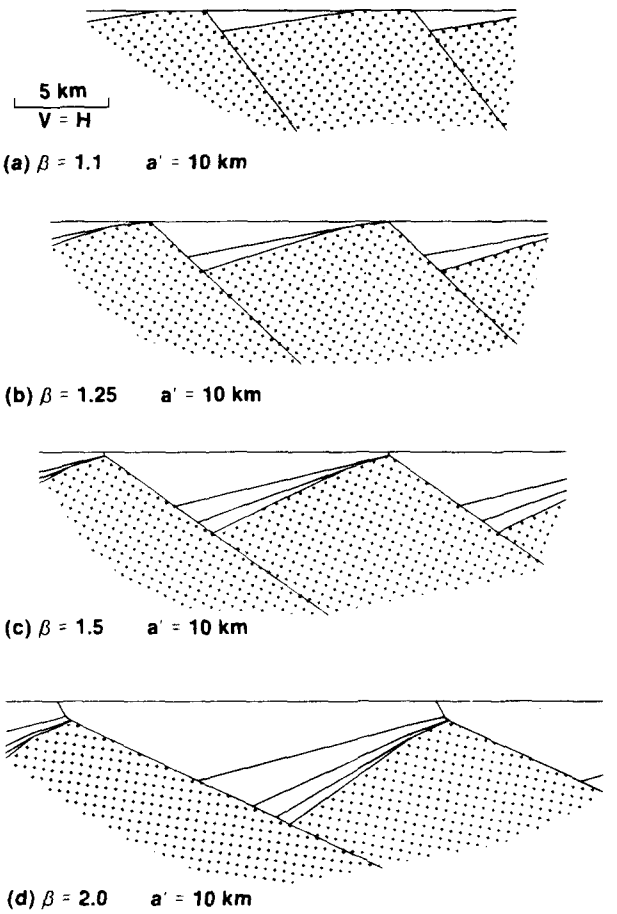

Fig. 8. Model set of half-grabens, derived for the isostatically compensated basin of Fig. 7 with an initial fault-plane dip of 60°. The horizontal line is sea-level, and basement is ornamented. (a)–(d) represent successive stages in the evolution of a basin with initial (pre-stretching) fault-plane spacing a' = 10 km. Sea-level markers from the previous steps have been extended with the basement to represent stratigraphic horizons, and are corrected for compaction within the sediment column. See text for further explanation.

In this example, early footwall uplift and erosion imparts a characteristic rounded 'shoulder' to the fault block (Fig. 8a). This is typical of many fault blocks in extensional terrains (e.g. Bowen 1975, fig. 2, Montadert *et al.* 1979). As overall subsidence outpaces relative footwall uplift, sediments onlap up the flank of the developing half-graben (Fig. 8b). When they reach the basement footwall cutoff, the fault must propagate upwards into the sediment column as a normal growth fault (Fig. 8c). If this fault is initiated at a constant dip relative to the sea bed (controlled by the mechanical properties of the sediment column, and assumed to be 60° in Fig. 8), it will take on a listric shape as early-formed segments are rotated to progressively lower angles (Fig. 8d). If smaller and more realistic increments of extension were chosen, both the footwall erosion surface and the growth fault would define smooth curves rather than the straight-line segments shown. However, where (as in this example) there is a period of non-deposition or erosion at the footwall cutoff, an angular discontinuity will remain between the planar basement segment of the

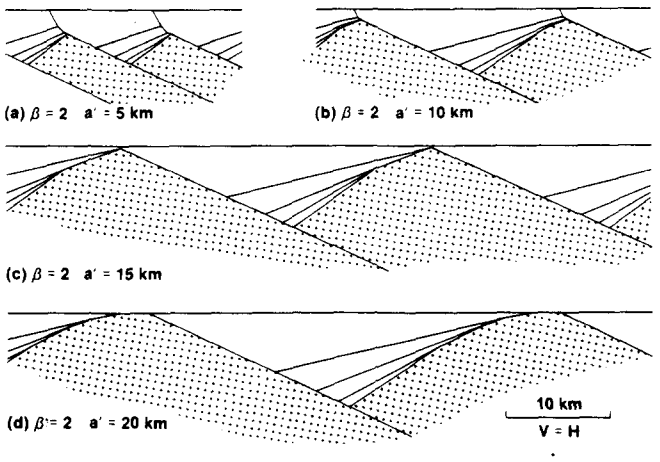

Fig. 9. Model set of half-grabens, constructed as in Fig. 8 and intended to show the effect of varying the initial fault-plane spacing a'. See text for further explanation.

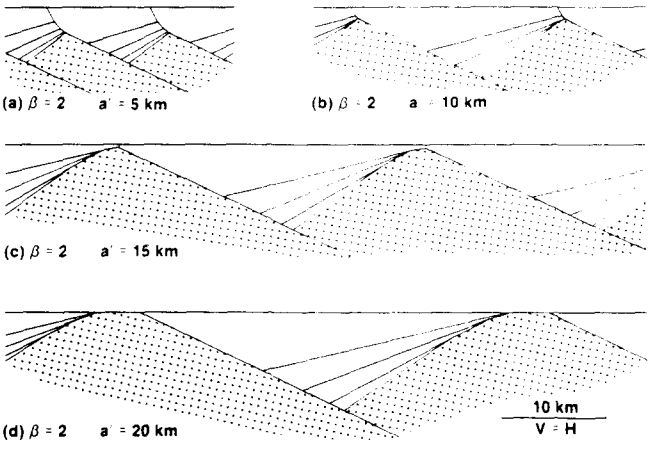

Fig. 10. Model set of half-grabens, constructed as in Fig. 9 but for a thin-skinned uncompensated basin with a sole fault at 7.5 km below sea-level. The models have been extended to $\beta = 2$ in order to facilitate comparison with Fig. 9, but such large extensions are unrealistic for (c) and (d) since the hangingwall would intersect the sole fault at $\beta = 1.8$ and $\beta = 1.6$ respectively. See text for further explanation.

fault surface and the upper listric segment. This angular difference reflects the rotation undergone by the basement fault plane while the crest of the fault block lay at or above sea-level.

Figure 9 shows a series of model half-grabens produced by the same procedure as Fig. 8(d), but with various initial fault spacings a'. Where $a' = 5$ km (Fig. 9a), footwall subsidence is continuous and the resulting listric growth fault passes smoothly into a planar fault at depth. However, the contrast in stratigraphic thickness between footwall and hangingwall is greatest for the oldest sedimentary package. The curvature of the growth fault is slightly exaggerated by compaction within the sediment column (cf. Jones & Addis 1984). Figure 9(b) is identical to Fig. 8(d). Where a' is increased above 10 km (Figs. 9c & d), the rate of onlap is reduced, footwall erosion is more severe and for the largest fault spacings, no growth fault forms and basement is exposed at sea-level throughout the stretching episode. In a fossil basin, the geometries of Fig. 9 will be modified by compaction of the syn-rift sediments during deposition of later sag-basin sediments, and perhaps by regional tilting as flexural processes gained in importance during the later stages of thermal subsidence (Dewey 1982).

Uncompensated basins. Figure 10 has been constructed to contrast the behaviour of compensated and uncompensated basins. The physical depth to decollement has been set at 7.5 km, in order that the total subsidence at $\beta = 2$ will be similar to that displayed by a compensated basin. The model half-grabens are very similar to those of Fig. 9. However, because the physical decollement remains at 7.5 km throughout the stretching episode (cf. the compensated basin model, where the notional depth to decollement lies at shallower depths during the early increments of stretching), early subsidence is more rapid in the uncompensated model. As a result, footwall erosion is less severe for a given initial fault spacing, and the earlier stratigraphic wedges are thicker and more extensive: for example there is only slight footwall erosion where $a' = 10$ km. In general, of course, the sole fault in an uncompensated basin is likely to take some other depth, resulting in either more or less uplift and erosion. An indication can be obtained of possible half-graben geometries by scaling all linear dimensions in terms of the depth to decollement: for example, the half-graben produced by an initial fault spacing of 20 km above a sole fault at 15 km depth would be geometrically similar to Fig. 10(b), formed with a fault spacing of 10 km above a sole fault at 7.5 km. The geometry of stratigraphic markers would not be identical, however, because the compaction law applied is exponential rather than linear. Uncompensated basins with very deep decollements, such as the Inner Moray Firth (20–25 km, Barr 1985, in press), will display only limited footwall uplift, even at very large fault spacings.

DISCUSSION

None of the models presented in this section should be regarded as an attempt to duplicate precisely the geometry of specific half-grabens in the geological record. The main intention is to demonstrate the variety of phenomena that can be generated by the simplest possible stretching model, and to identify the major controlling parameters. Nevertheless, it is possible to recognise broad analogies between structures recorded on seismic reflection surveys and the models in Figs. 9 and 10. The Brent oilfield structure (Bowen 1975) and fault blocks on the Armorican continental margin (Montadert *et al.* 1979) are comparable to Fig. 9(d), Heather field (Gray & Barnes 1981) to Fig. 9(c) and Beatrice field (Linsley *et al.* 1980) to Fig. 10(a) (although with less extension, and scaled by a factor of three to incorporate the deep Inner Moray Firth decollement).

The main conclusion to be drawn from the models is that simple uniform stretching can generate quite complex uplift/subsidence histories at the readily accessible up-dip ends of half-grabens: not only uplift *or* subsidence

depending on the parameters chosen, but uplift *and* subsidence of an individual reference point on a fault block. A subsidiary result of some importance is that listric normal growth-faulting can be produced in the sediment cover by a fundamentally planar process of extensional faulting. In the most general case, a simple extensional half-graben will record a history of early uplift, erosion and regression, subsequent transgression and onlap, and finally submergence of the footwall island with the formation of a listric growth fault. Depending on the specific parameters chosen, individual half-grabens may undergo only part of this history (e.g. uplift only; growth faulting only; uplift and onlap only). Uplift is favoured and subsidence inhibited by: (i) a shallow depth to decollement, either notional (compensated) or physical (uncompensated); (ii) a steep initial fault-plane dip; or (iii) a large initial fault-plane spacing. Other factors that have not been considered include: (i) the possibility of slow or inhomogeneous stretching, which would modify the overall subsidence rate and hence the notional depth to decollement; (ii) local modification of the overall subsidence rate by lithospheric flexure resulting from partial isostatic compensation (e.g. inhibition of subsidence as a flexural bulge passed a specified fault block); (iii) alternative mechanisms of upper crustal faulting, which in general give rise to less structural relief than the domino model and hence less footwall uplift; (iv) local isostatic effects, which modify the fault-block geometry and in general favour footwall uplift (e.g. Jackson & McKenzie 1983); and (v) deviations from the simple tectonosedimentary model chosen (e.g. footwall islands may not have been eroded down to sea-level, the syn-rift sediments may not completely fill the half-grabens, and steep fault scarps may fail on secondary detachments). At large extensions, the possibility also exists that early faults, rotated to low angles, will be abandoned and reworked by a new set of high-angle faults (e.g. Proffett 1977). This would effectively rejuvenate the system and give rise to a renewed episode of active footwall uplift.

CONCLUSIONS

Analysis of the equations that describe homogeneous isostatically compensated lithospheric stretching permits the definition of a level of no vertical motion during stretching. This level is controlled by the mean density of the basin fill, and for a water-loaded basin lies at a depth of about 3.3 km and coincides with the level to which the asthenosphere would rise if loaded by sea-water only: that is, to the mantle geoid. In general, the physical sole to a system of detached upper-crustal normal faults will not lie at this level and must move vertically (as a passive marker undergoing pure shear) during stretching. Such movement limits the usefulness of area (or volume) balancing techniques as a means of determining the depth to a physical decollement. If allowance is not made for the vertical movement of the sole fault, such calculations will yield the depth to the level of no vertical motion. In view of this relationship, and the fact that the level of no vertical motion itself moves vertically in a sediment-filled basin as sediment compaction causes increased isostatic loading, it has been proposed (Barr 1987) that the term notional depth to decollement be used for this purely conceptual parameter. By reference to the notional depth to decollement, it is possible to simplify descriptions of subsidence in isostatically compensated extensional basins, and to show that in most situations, individual parameters such as crustal thickness have a very limited influence on the magnitude of basement subsidence during homogeneous stretching. In contrast, subsidence (sediment volume or cross-sectional area) in thin-skinned uncompensated basins is controlled directly by the depth to the physical sole fault and is independent of the density of the basin fill. In uncompensated basins (usually recognizable by the presence of a large negative gravity anomaly) section-balancing techniques should yield the true depth to decollement.

Absolute footwall uplift in a system of upper crustal fault blocks can be determined from the relative magnitudes of overall basin subsidence and basement relief due to faulting. For the simplest model, involving domino-style faulting, uplift of footwall islands above sea-level is favoured by a large initial (pre-stretching) fault spacing, a steep initial fault-plane dip and a large physical (in an uncompensated basin) or notional (in a compensated basin) depth to decollement. For a given set of parameters and a chosen maximum value of the stretching factor β, four fields can be defined on the basis of initial fault-plane dip and spacing: one in which basement footwall cutoffs always subside relative to sea-level; one in which they are uplifted above sea-level and then subside below sea-level; one in which they are uplifted and then subside but remain above sea-level; and one in which they are always uplifted.

An understanding of footwall uplift is of considerable relevance to exploration for hydrocarbons because the upper flanks of half-grabens are among the most accessible, economically attractive and thoroughly explored parts of sedimentary basins. Their uplift histories will particularly affect the extent to which pre-rift sediments have been eroded across the crests of fault blocks, and the facies of nearby syn-rift sediments. Two sets of model half-grabens have been presented, one for an uncompensated basin with a sole fault at 7.5 km depth and one for a compensated basin loaded by clastic sediments having an exponential compaction/depth relationship. Perhaps the most important generalisation that can be made is that simple progressive extension can give rise to a wide variety of structural and stratigraphic features, either from one fault block to the next or throughout the history of an individual fault block. Regression (erosion of footwall basement and reworking of early syn-rift sediments), transgression (onlap up the flank of a half-graben), and simple growth faulting can all be predicted. In the latter case, listric faults within the cover pass, with or without angular discordance, into lower-angle planar faults within the basement. This geometry, which can be purely extensional, has often

been attributed to extensional reactivation of basement thrusts (e.g. compare Brewer & Smythe 1984 with Wernicke *et al.* 1985). In general, carefully integrated studies of tectonic and stratigraphic relationships are required to distinguish the products of continuous extension from those of other phenomena such as regional uplift or pre-rift thermal doming, alternating compression and extension, and eustatic sea-level changes.

Acknowledgements—The work reported here was carried out at the British Geological Survey, under the auspices of the Spatial Modelling Research Programme. It is published with the approval of the Director, British Geological Survey and by permission of Britoil plc.

REFERENCES

Badley, M. E., Egeberg, T. & Nipen, O. 1984. Development of rift basins illustrated by the structural evolution of the Oseberg feature, Block 30/6, offshore Norway. *J. geol. Soc. Lond.* **141**, 639–649.

Barr, D. 1985. 3-D palinspastic restoration of normal faults in the Inner Moray Firth: implications for extensional basin development. *Earth Planet. Sci. Lett.* **75**, 191–203.

Barr, D. 1987. Lithospheric stretching, detached normal faulting and footwall uplift. In: *Continental Extensional Tectonics* (edited by Coward, M. P., Dewey, J. F. & Hancock, P. L.). *Spec. Publ. geol. Soc. Lond.* In press.

Barr, D., McQuillin, R. & Donato, J. A. 1985. Footwall uplift in the Inner Moray Firth basin, offshore Scotland. *J. Struct. Geol.* **7**, 267–268.

Barton, P. & Wood, R. 1984. Tectonic evolution of the North Sea basin: crustal stretching and subsidence. *Geophys. J. R. astr. Soc.* **79**, 987–1022.

Bosworth, W. 1985. Discussion on the structural evolution of extensional basin margins. *J. geol. Soc. Lond.* **142**, 939–940.

Bowen, J. M. 1975. The Brent oil-field. In: *Petroleum and the Continental Shelf of North-west Europe* (edited by Woodland, A. W.). Applied Science, London. 353–360.

Brewer, J. A. & Smythe, D. K. 1984. MOIST and the continuity of crustal reflector geometry along the Caledonian–Appalachian orogen. *J. geol. Soc. Lond.* **141**, 105–120.

Chapman, T. J. & Williams, G. W. 1984. Displacement–distance methods in the analysis of fold-thrust structures and linked-fault systems. *J. geol. Soc. Lond.* **141**, 121–128.

Chenet, P., Montadert, L., Gairaud, H. & Roberts, D. 1983. Extension ratio measurements on the Galicia, Portugal and northern Biscay continental margins: implications for evolutionary models of passive continental margins. In: *Studies in Continental Margin Geology* (edited by Watkins, J. S. & Drake, C. L.). *Am. Ass. petrol. Geol. Mem.* **34**, 703–715.

Cochran, J. R. 1983. Effects of finite rifting times on the development of sedimentary basins. *Earth Planet. Sci. Lett.* **66**, 289–302.

Dahlstrom, C. D. A. 1969. Balanced cross-sections. *Can. J. Earth Sci.* **6**, 743–757.

Dewey, J. F. 1982. Plate tectonics and the evolution of the British Isles. *J. geol. Soc. Lond.* **139**, 371–412.

Donato, J. A. & Tully, M. C. 1981. A regional interpretation of North Sea gravity data. In: *Petroleum Geology of the Continental Shelf of North-west Europe* (edited by Illing, L. V. & Hobson, G. D.). Institute of Petroleum, London. 65–75.

Froidevaux, C. 1986. Basin and range large-scale tectonics; constraints from gravity and reflection seismology. *J. geophys. Res.* **91**, 3625–3632.

Gibbs, A. D. 1983. Balanced cross-section construction from seismic sections in areas of extensional tectonics. *J. Struct. Geol.* **5**, 471–482.

Gibbs, A. D. 1984. Structural evolution of extensional basin margins. *J. geol. Soc. Lond.* **141**, 609–620.

Gibbs, A. D. 1985. Discussion on the structural evolution of extensional basin margins. *J. geol. Soc. Lond.* **142**, 940–942.

Gray, W. D. T. & Barnes, G. 1981. The Heather oil field. In: *Petroleum Geology of the Continental Shelf of North-West Europe* (edited by Illing, L. V. & Hobson, G. D.). Institute of Petroleum, London. 335–341.

Hellinger, S. J. & Sclater, J. G. 1983. Some comments on two-layer extensional models for the evolution of sedimentary basins. *J. geophys. Res.* **88**, 8251–8269.

Hutchinson, D. R., Klitgord, K. D. & Detrick, R. S. 1986. Rift basins of the Long Island Platform. *Bull. geol. Soc. Am.* **97**, 688–702.

Jackson, J. A. & McKenzie, D. 1983. The geometrical evolution of normal fault systems. *J. Struct. Geol.* **5**, 471–482.

Jarvis, G. T. 1984. An extensional model of graben subsidence—the first stage of basin evolution. *Sediment. Geol.* **40**, 13–31.

Jones, M. E. & Addis, M. A. 1984. Volume change during sediment diagenesis and the development of growth faults. *Marine petrol. Geol.* **1**, 118–122.

Le Pichon, X., Angelier, J. & Sibuet, J. C. 1982. Plate boundaries and extensional tectonics. *Tectonophysics* **81**, 239–256.

Le Pichon, X., Angelier, J. & Sibuet, J. C. 1983. Subsidence and stretching. In: *Studies in Continental Margin Geology* (edited by Watkins, J. S. & Drake, C. L.). *Am. Ass. petrol. Geol. Mem.* **34**, 731–741.

Le Pichon, X. & Sibuet, J. C. 1981. Passive margins: a model of formation. *J. geophys. Res.* **86**, 3708–3720.

Linsley, P. M., Potter, H. C., McNab, J. & Racher, D. 1980. The Beatrice Field, Inner Moray Firth. In: *Giant Oil and Gas Fields of the Decade 1968–1978* (edited by Halbouty, M. T.). *Am. Ass. Petrol. Geol.*, Tulsa. 117–129.

McKenzie, D. 1978. Some remarks on the development of sedimentary basins. *Earth Planet. Sci. Lett.* **40**, 25–32.

McKenzie, D. 1981. The variation of temperature with time and hydrocarbon maturation in sedimentary basins formed by extension. *Earth Planet. Sci. Lett.* **55**, 87–98.

McKenzie, D. 1984. A possible mechanism for epeirogenic uplift. *Nature, Lond.* **307**, 616–618.

McQuillin, R., Donato, J. A. & Tulstrup, J. 1982. Development of basins in the Inner Moray Firth and the North Sea by crustal extension and dextral displacement of the Great Glen Fault. *Earth Planet. Sci. Lett.* **60**, 127–139.

Montadert, L. Roberts, D. G., de Charpal, O. & Guennoc, P. 1979. Rifting and subsidence of the northern continental margin of the Bay of Biscay. In: *Initial Reports of the Deep Sea Drilling Project* (edited by Montadert, L., & Roberts, D. G.). U.S. Government Printing Office, Washington, DC **48**, 1025–1060.

Parsons, B. & Sclater, J. C. 1977. An analysis of the variation of ocean floor bathymetry and heat flow with age. *J. geophys. Res.* **82**, 803–827.

Proffett, J. M. 1977. Cenozoic geology of the Yerington district, Nevada, and implications for the nature of Basin and Range faulting. *Bull. geol. Soc. Am.* **88**, 247–266.

Royden, L., Horvath, F., Nagymarosy, A. & Stegena, L. 1983. Evolution of the Pannonian basin system. 2. Subsidence and thermal history. *Tectonics* **2**, 91–137.

Royden, L. & Keen, C. E. 1980. Rifting process and thermal evolution of the continental margin of eastern Canada determined from subsidence curves. *Earth Planet. Sci. Lett.* **51**, 343–361.

Sclater, J. G. & Christie, P. A. F. 1980. Continental stretching: an explanation of the post-mid-Cretaceous subsidence of the Central North Sea. *J. geophys. Res.* **85**, 3711–3739.

Steckler, M. S. 1985. Uplift and extension at the Gulf of Suez: indications of induced mantle convection. *Nature, Lond.* **317**, 135–139.

Steckler, M. S. & Watts, A. B. 1978. Subsidence of the Atlantic-type continental margin off New York. *Earth Planet. Sci. Lett.* **41**, 1–13.

Turcotte, D. L., Haxby, W. F. & Ockendow, J. R. 1977. Lithospheric instabilities. In: *Island Arcs, Deep-Sea Trenches and Back-Arc Basins* (edited by Talwani, M. & Pitman, W. C.). *Am. geophys. Union M. Ewing Series* **1**, 63–69.

Ussami, N., Karner, G. D. & Bott, M. H. P. 1986. Crustal detachment during South Atlantic rifting and formation of Tucano–Gabon basin system. *Nature, Lond.* **332**, 629–632.

Wernicke, B. 1981. Low-angle normal faults in the Basin and Range Province—nappe tectonics in an extending orogen. *Nature, Lond.* **291**, 645–648.

Wernicke, B. 1985. Uniform normal-sense simple shear of the continental lithosphere. *Can. J. Earth Sci.* **22**, 108–125.

Wernicke B. & Burchfiel, B. C. 1982. Modes of extensional tectonics. *J. Struct. Geol.* **4**, 105–115.

Wernicke B., Walker, J. D. & Beaufait, M. S. 1985. Structural discordance between Neogene detachments and frontal Sevier thrusts, Central Mormon Mountains, Southern Nevada. *Tectonics* **4**, 213–246.

Yuen, D. A. & Fleitout, L. 1985. Thinning of the lithosphere by small-scale convective destabilisation. *Nature, Lond.* **313**, 125–128.